SCIENCE CHINA
Earth Sciences

•REVIEW•

February 2023 Vol.66 No.2: 190–204
https://doi.org/10.1007/s11430-022-1007-5

Destruction of the lower crust beneath the North China Craton recorded by granulite and pyroxenite xenoliths

Dongya ZOU[1*] & Hongfu ZHANG[1,2]

[1] *School of Earth Sciences, Zhejiang University, Hangzhou 310027, China;*
[2] *Department of Geology, Northwest University, Xi'an 710069, China*

Received January 31, 2022; revised August 15, 2022; accepted September 13, 2022; published online December 16, 2022

Abstract The lower crust beneath the North China Craton (NCC) was transformed during the craton destruction in the Mesozoic, however, the transformation processes are yet to be fully understood. Compositional and geochronological variations of granulite and pyroxenite xenoliths provided insights into the nature of the lower crust before and after the craton destruction. In this study, we summarized the latest results of geochemistry and zircon geochronology coupled with Hf-O isotopes from granulite and pyroxenite xenoliths hosted by Phanerozoic igneous rocks in NCC. Comparing previous studies on the granulite terranes and adakitic rocks of NCC, we aim to discuss the destruction processes of lower crust beneath the NCC. The granulite and pyroxenite xenoliths of NCC were divided into two and three groups, respectively, based on the differences of geochemical features. Group I granulite xenoliths from the NCC have silicic-basic compositions, with metamorphic ferrosilite. The Group I granulite xenoliths show relatively lower Mg# values of pyroxenes and whole-rock than that of the Group II granulite xenoliths, and enrichments of light rare earth elements and Sr-Nd isotopic compositions. Their zircons display Archean-Phanerozoic ages with three peaks of Neoarchean, Paleoproterozoic, and Mesozoic. Generally, Group I granulite xenoliths show close affinities to the granulite terranes of the NCC in terms of the major and trace elements and Sr-Nd isotopic compositions, with a consistent Archean-Proterozoic evolutionary history. However, Group I granulite xenoliths have abundant Phanerozoic zircons with variable Hf isotopic compositions from depleted to enriched, which could be formed by modifications of magma underplating. Therefore, Group I granulite xenoliths represent the modified ancient lower crust beneath the NCC. The Group II granulite and Group III pyroxenite xenoliths from the NCC have similar geochemical features and are basic in compositions, with metamorphic to magmatic orthopyroxenes. The Group II granulite and Group III pyroxenite xenoliths usually show higher MgO and lower incompatible elements compositions in minerals and bulk rocks than that in the granulite terranes and Group I granulite xenoliths, but their Sr-Nd isotopic compositions fall into the fields of granulite terranes and group I granulite xenoliths. Zircons from the Group II granulite and Group III pyroxenite xenoliths are predominantly Phanerozoic with subordinate Archean-Proterozoic ages, and the Hf-O isotopic compositions of zircons are similar to those in the Group I granulite xenoliths. Additionally, the trace element compositions of Group II granulite and Group III pyroxenite xenoliths are complementary to those of the adakitic rocks from the NCC. Furthermore, the similar Sr-Nd and zircon Hf isotopic compositions among Group II granulite and Group III pyroxenite xenoliths and adakitic rocks indicate that they are cognate. Therefore, we suggest that the Group II granulite and Group III pyroxenite xenoliths could be restites left after partial melting of the ancient basic lower crust that produced voluminous adakitic rocks. In contrast, Group I and II pyroxenite xenoliths from the NCC have cumulate and reaction origins, respectively. The Group I and II pyroxenite xenoliths commonly have magmatic enstatite and show higher Mg# values and depleted Sr-Nd isotopic compositions of minerals and bulk rocks relative to that in the granulite and Group III pyroxenite xenoliths. Formation of voluminous Group I pyroxenite cumulates in the crust-mantle transition zones implies extensive magma underplating beneath the NCC during the Mesozoic-Cenozoic, which also provided exotic materials and heat for the reworking of the ancient lower crust. Therefore, the destruction of the lower crust beneath the NCC could result from continuous modifications and remelting of the ancient lower crust triggered by magma underplating. These processes led to not only the transformations of some ancient basic lower crust into granulite and pyroxenite restites but also the compositional

* Corresponding author (email: zoudongya@zju.edu.cn)

modifications of the ancient lower crust. Consequently, the lower crust beneath the NCC showed downward rejuvenation, similar to the lithospheric mantle.

Keywords North China Craton, Destruction of lower crust, Granulite xenolith, Pyroxenite xenolith

Citation: Zou D, Zhang H. 2023. Destruction of the lower crust beneath the North China Craton recorded by granulite and pyroxenite xenoliths. Science China Earth Sciences, 66(2): 190–204, https://doi.org/10.1007/s11430-022-1007-5

1. Introduction

The lower crust is an important layer of the earth that records crust-mantle interactions and is the source of intermediate-silicic magmas, thus, it is crucial to understand the composition and structure of lower continental crust. The North China Craton (NCC) has been widely studied with respect to the pronounced changes in its lithosphere from a thick, cool, and refractory lithosphere in the Paleozoic to a thin, hot, and fertile lithosphere in the Cenozoic (Menzies et al., 1993; Griffin et al., 1998; Fan et al., 2000; Zhai, 2008; Zhang, 2009; Wu et al., 2014; Li and Wang, 2018; Wang K et al., 2018; Wang Y et al., 2018; Zheng et al., 2018; Zhu and Xu, 2019). The lithospheric mantle and lower crust beneath the NCC were variably thinned and transformed during the craton destruction (Zhai et al., 2007; Ying et al., 2013a; Zheng et al., 2021b). Mechanisms of thinning and transformation of the lithospheric mantle beneath the NCC have reached a broad consensus (Zhang, 2009; Zong and Liu, 2018; Tang et al., 2021; Zheng et al., 2021a). However, the destruction processes of the lower crust beneath the NCC remain controversial. Several compelling models have been proposed, such as the delamination of the basic lower crust (Gao et al., 2004; Deng et al., 2006; Xu et al., 2013), and underplating and replacement (Zhai et al., 2007; Zheng et al., 2021b). In contrast, some studies of the Mesozoic adakitic rocks argued against the delamination of the lower crust beneath the NCC (Chen et al., 2012; Qian and Hermann, 2013; Ma et al., 2015). Moreover, it has been controversial whether the magmatic underplating formed the newly accreted basic granulite (Liu et al., 2004a; Zheng et al., 2009b; Ma et al., 2017) or simply led to the remelting of the ancient lower crust during the Phanerozoic (Jiang and Guo, 2010; Hu et al., 2020).

In addition to geophysical methods, the Precambrian granulite terranes, lower crustal xenoliths entrained in basaltic or kimberlitic rocks, and crust-derived volcanic rocks provide information on the lower crust (Zhai and Guo, 1992; Liu et al., 2001, 2004a, 2004b; Zhai and Liu, 2001; Rudnick and Gao, 2014; Zheng et al., 2021b). The widespread Precambrian granulite terranes exposed in the NCC represent the lower crust before its destruction. Granulite and pyroxenite xenoliths carried by the Phanerozoic magmatic rocks of the NCC provide direct samples for investigating the composition, nature, and evolution of the lower crust before and after the destruction (Figure 1). Extensive Mesozoic adakitic intermediate-silicic magmatic rocks in the NCC are associated with magma underplating and melting of the basic lower crust, thus, can also inverse the evolution of lower crust beneath the NCC. Numerous studies have been conducted on the granulite terranes, granulite and pyroxenite xenoliths and adakitic rocks from the NCC (Chen et al., 2001; Liu et al., 2001, 2004a, 2005, 2020; Xu, 2002; Zhang et al., 2003; Zheng et al., 2003, 2004a, 2004b, 2009a, 2009b, 2012; Huang et al., 2004; Jiang and Guo, 2010; Ying et al., 2010; Shao and Wei, 2011; Xu et al., 2013; Ying et al., 2013b; Hu et al., 2016; Ma et al., 2017, 2020; Zhao et al., 2017, 2021; Wei et al., 2019; Dai et al., 2021). In this work, we summarized the latest geochemical and geochronological results of granulite and pyroxenite xenoliths and compared with that of granulite terranes and adakitic rocks to explore the destruction processes of the lower crust beneath the NCC.

2. Composition and evolution of the lower crust recorded by granulite terranes

The Precambrian granulite terranes represent the lower crust beneath the NCC before the craton destruction. The granulite terranes are primarily distributed in the Trans-North China Orogen, Inner Mongolia Suture Zone, Yinshan Block, Jiao-Liao-Ji Belt, and Eastern Block (Figure 1) (Zhai, 2004; Zhao et al., 2005, 2012). They are felsic to basic granulites that are mainly composed of plagioclase, orthopyroxene, clinopyroxene, garnet, amphibole, and mica. Amphibole and mica were not discussed in this study due to the absence of hydrated minerals in the granulite xenoliths. Plagioclase in the granulite terranes is oligoclase-andesine, and garnet is almandine with pyrope constituent (Figure 2). Clinopyroxene in the granulite terranes is diopside-augite (Figure 2) with low Mg# values (Figure 3a and 3b), and orthopyroxene is predominantly metamorphic ferrosilite (Figures 2 and 3) with low Mg# values (Figure 3c) (Zhang et al., 1982; Jin and Li, 1986; Cui et al., 1991; Cui and Wang, 1992; Liu, 1997; Guo et al., 1998, 2005; Huang et al., 2001). Granulite terranes show variable SiO_2 contents, Mg# values and Sr-Nd isotopic compositions (Figures 4 and 6), and uniform light rare earth element (LREE)-enriched patterns (Figure 5a). Granulite terranes in the Trans-North China Orogen, Inner Mongolia Suture and Jiao-Liao-Ji Belt formed mainly in the

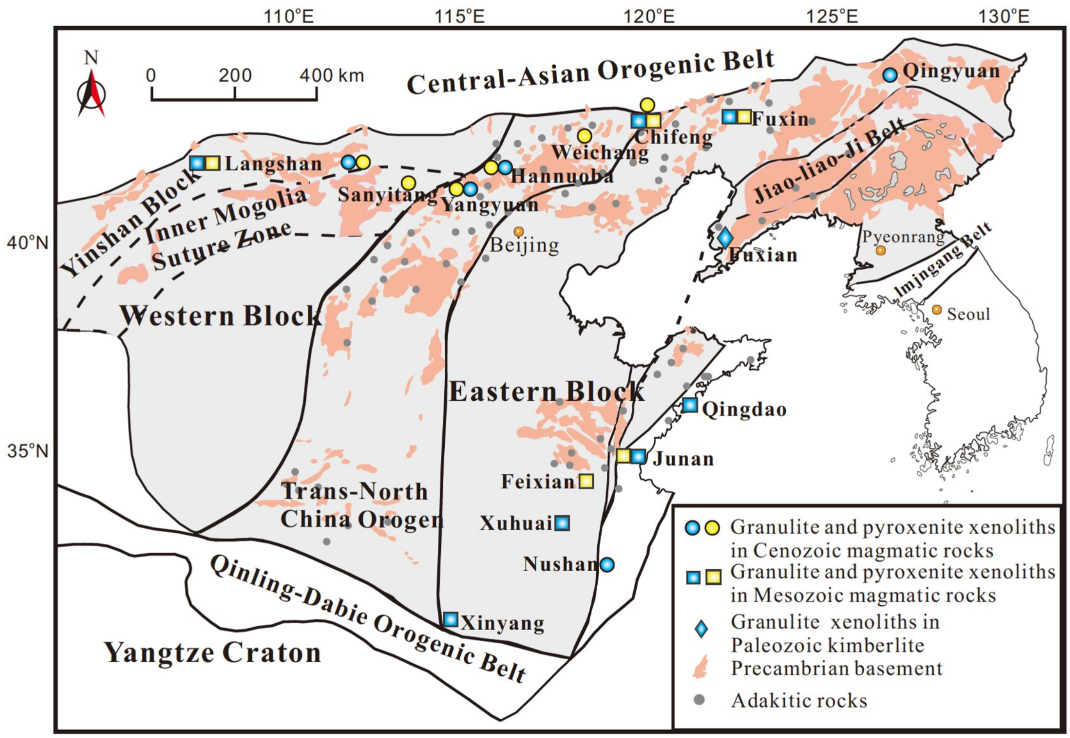

Figure 1 Distribution of the Precambrian granulite terranes, Phanerozoic granulite and pyroxenite xenoliths, and adakitic rocks in the NCC (modified from Zhao et al. (2005) and Zhang et al. (2001b)).

Paleoproterozoic with a clockwise pressure-temperature-time (*P-T-t*) path. Granulite terranes in the Yinshan Block and Eastern Block formed mainly in the Archean with an anticlockwise *P-T-t* path (Guo and Zhai, 2000; Guo et al., 2001; Zhao et al., 2005, 2012; Zhai, 2009). In addition, the Archean granulite terranes in the Eastern Block often demonstrate overprinting of Late Paleoproterozoic high-pressure granulite facies metamorphism (Yang and Wei, 2017; Wei, 2018; Lu and Wei, 2020; Xu et al., 2021). Basic garnet granulite terranes represent the lowermost lower crust and display metamorphic pressure of ⩾1.15 GPa, implying that the crust of the NCC was at least ~40 km thick in the Precambrian (Zhai et al., 2007; Zhai, 2008).

3. Composition and evolution of the lower crust recorded by granulite xenoliths

Granulite xenoliths in the Phanerozoic magmatic rocks represent different periods lower crust beneath the NCC and have different geological implications. Granulite xenoliths hosted by the Fuxian kimberlite (~480 Ma) are basic garnet granulite, which formed in 2.7–2.5 Ga and underwent tectonic and thermal reworking during the Paleoproterozoic (1.9–1.8 Ga) and Neoproterozoic (700–600 Ma) (Zheng et al., 2004b). Geochemical features of the primary minerals in the Fuxian granulite xenoliths are similar to those of the garnet granulites from the NCC granulite terranes (Zheng et al., 2004b). Thus, the Fuxian granulite xenoliths represent the lower crust beneath the NCC before the craton destruction.

Abundant granulite xenoliths entrained in the Mesozoic-Cenozoic magmatic rocks from the NCC are located in its northern and southeastern margins (Figure 1). Various lower crust-derived xenoliths from the Xinyang (~160 Ma) and Xuhuai (~132 Ma) regions within the southeastern NCC (Figure 1) have been studied, including amphibolite, granulite, and eclogite. Equilibrium pressures of the garnet granulite and eclogite xenoliths suggest that the crust of the southeastern NCC was at least 45 km thick in the Late Mesozoic (Zheng et al., 2003; Xu et al., 2006a). The Xinyang granulite xenoliths formed in 3.8–3.6 Ga, and experienced multiple reworking and accretion at ~3.5, ~2.5, and ~1.8 Ga, respectively (Zheng et al., 2004a; Ping et al., 2015; Ma et al., 2020). The Xuhuai granulites formed in 2.5–2.4 Ga and experienced high pressure granulite-facies metamorphism in ~1.8 Ga (Liu Y C et al., 2009). However, granulite xenoliths from the Qingdao (~86 Ma), Junan (~67 Ma), and Nushan (~1 Ma) regions within the southeastern NCC (Figure 1) are primarily garnet-absent silicic to basic compositions, with the exception of minor garnet granulite xenoliths in the Junan region. Equilibrium pressures of the granulite xenoliths from the Qingdao, Junan and Nushan regions imply that the crust of the southeastern NCC was no more than 35 km thick during the Late Mesozoic-Cenozoic (Huang et al., 2004; Zhang and Zhang, 2007; Ying et al., 2010). Granulite xe-

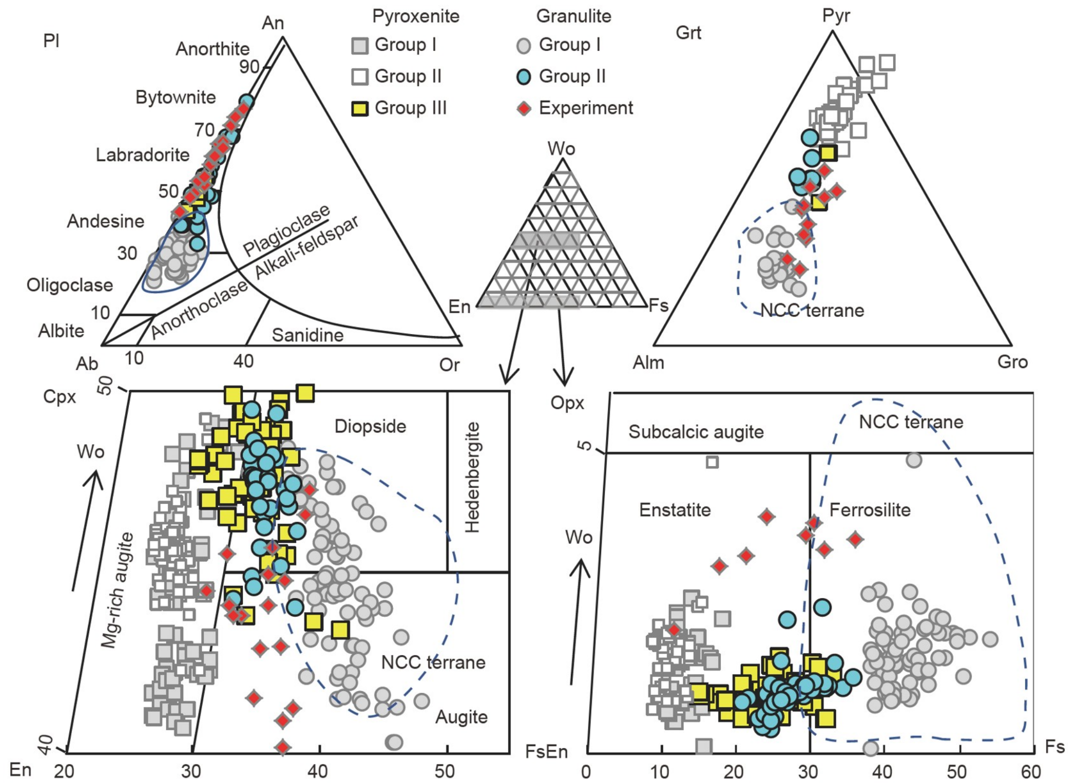

Figure 2 Ternary diagrams of Ab-An-Or for plagioclase, Alm-Pyr-Gro for garnet and En-Wo-Fs for pyroxene. Data sources: granulite xenoliths (Fan and Liu, 1996; Chen et al., 2001; Liu et al., 2003; Liu Y C et al., 2009; Zheng et al., 2003, 2004c, 2009b; Huang et al., 2004; Zhang and Zhang, 2007; Jiang and Guo, 2010; Ying et al., 2010; Du and Fan, 2011; Zhang et al., 2016; Ma et al., 2017), Group I and II granulite xenoliths represent modified ancient lower crust and partial melting residues of ancient basic lower crust, respectively; pyroxenite xenoliths (Liu et al., 2004b; Zhang et al., 2007; Zheng et al., 2009b; Shao and Wei, 2011; Xu et al., 2013; Ying et al., 2013b; Zou et al., 2014; Hu et al., 2016; Zhao et al., 2017, 2021; Wei et al., 2019; Dai et al., 2021; Liu et al., 2020), Group I and II pyroxenite xenoliths have cumulate and reaction origin, respectively, and Group III pyroxenite xenoliths are residues of partial melting of ancient basic lower crust; granulite terranes (Zhang et al., 1982; Jin and Li, 1986; Cui et al., 1991; Liu, 1997; Guo et al., 1998, 2005; Huang et al., 2001; Yang and Wei, 2017; Lu and Wei, 2020; Xu et al., 2021); experimental data of partial melting of basic lower crust (Springer and Seck, 1997; Qian and Hermann, 2013). Pl, Plagioclase; Grt, Garnet; Opx, Orthopyroxene; Cpx, Clinopyroxene.

noliths from the Qingdao, Junan and Nushan regions formed mainly in the Neoarchean (2.7–2.5 Ga) and were modified by the Paleoproterozoic tectono-thermal events, which is consistent with the evolutionary history of the granulite terranes of the eastern NCC. However, numerous 140–90 Ma zircons with a large range of Hf isotopic compositions have been observed in the granulite xenoliths from the Qingdao, Junan and Nushan regions (Huang et al., 2004; Ying et al., 2010; Zhang, 2012; Ping et al., 2019). Ping et al. (2019) suggested that the basic granulites with Mesozoic ages from the Nushan region could be part of a newly accreted lower crust.

Granulite xenoliths in the Mesozoic-Cenozoic magmatic rocks from the northern margin of the NCC are widely distributed in Chifeng (~227 Ma), Siziwangqi (~128–108 Ma), Fuxin (~100 Ma), Hannuoba (27–14 Ma), and Qingyuan (~19 Ma). Most of granulite xenoliths from the northern margin of the NCC are garnet-absent granulites. Equilibrium pressures of the granulite xenoliths from the Siziwangqi in the Western Block and Hannuoba in the Trans-North China Orogen (Figure 1) indicate that the crustal thickness could reach 40 and 42 km in the area during the Cenozoic, respectively (Chen et al., 2001; Liu et al., 2001; He et al., 2009). However, equilibrium pressures of granulite xenoliths from the Chifeng and Fuxin regions in the northeastern NCC reflect a crustal thickness of <33 km in the Mesozoic (Shao and Wei, 2011; Ma et al., 2017; Zou and Zhang, 2022). This implies that the destruction of the lower crust beneath the northeastern NCC began earlier, making it thinner than that in the southeastern NCC. The intermediate-silicic granulite xenoliths from the Siziwangqi, Fuxin, Hannuoba, and Qingyuan regions formed in 2.7–2.5 Ga (He et al., 2009; Wei et al., 2015; Ma et al., 2020; Zou et al., 2022). ~1.8 Ga zircons in the Hannuoba granulite xenoliths indicate the influence of the Paleoproterozoic tectono-thermal event. In addition, all intermediate-silicic granulite xenoliths from the northern NCC contain abundant 220–45 Ma zircons with variable Hf isotopic compositions. However, most zircons in the basic granulite xenoliths from the Chifeng, Fuxin, and Hannuoba regions yielded ages of 315–83 Ma, with a few Archean-Proterozoic ages (Liu et al., 2004a; Zheng et al., 2009b; Shao et al., 2012; Ma et al., 2017). Some authors have suggested that the basic granulites with Phanerozoic ages were pro-

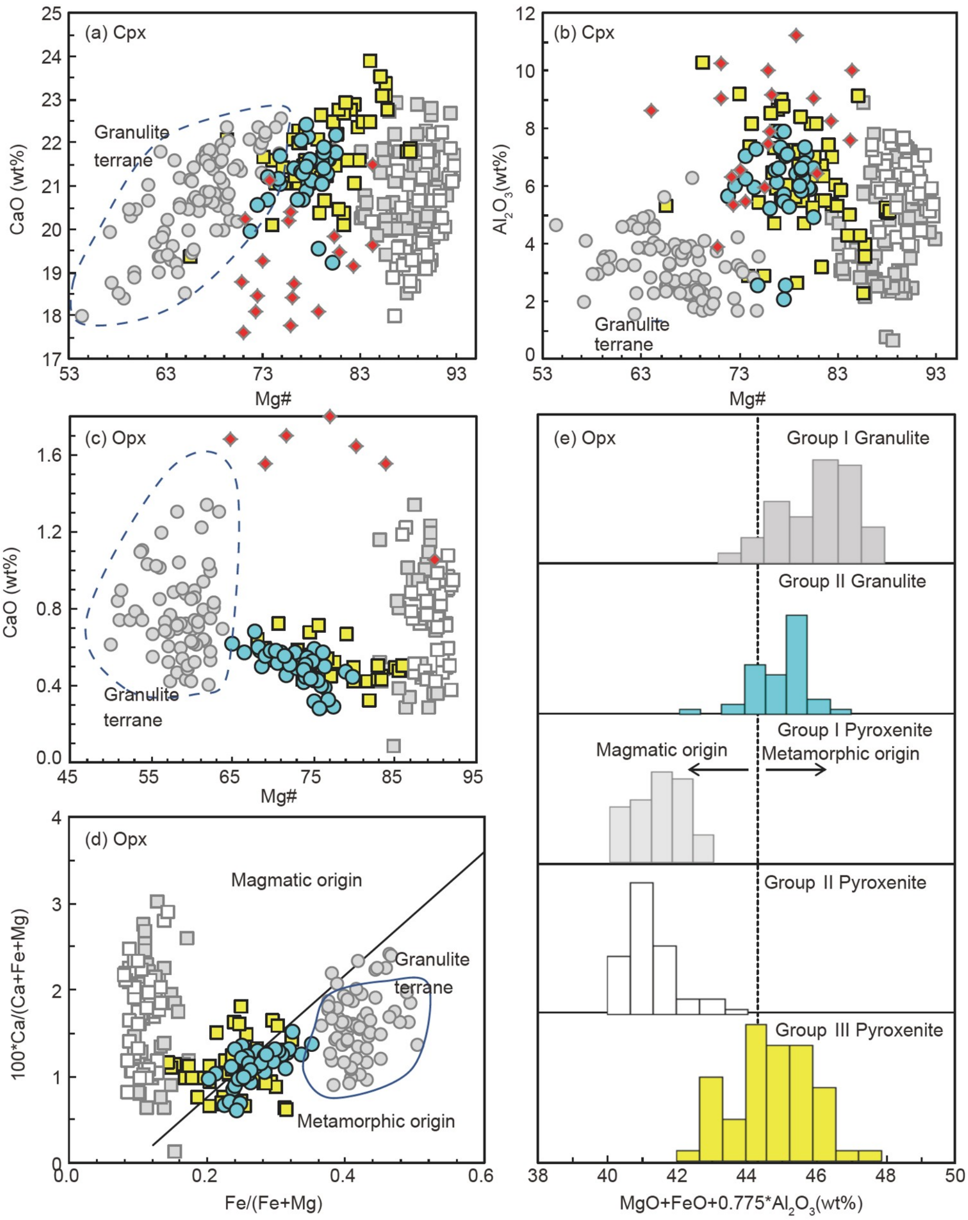

Figure 3 Diagrams for major element compositions of pyroxenes in granulite and pyroxenite xenoliths. Mg# vs. (a) CaO and (b) Al_2O_3 contents in Cpx; (c) Mg# vs. CaO content in Opx; ((d) and (e)) Discrimination diagram of orthopyroxene origin (Bhattacharyya, 1971; Rietmeijer, 1983). Symbols and data sources are the same as Figure 2.

ducts of magma underplating during the Phanerozoic (Zheng et al., 2009b, 2012; Ma et al., 2017), while others have suggested that some intermediate-basic granulite xenoliths from Hannuoba and Fuxin are residues of partial melting of an ancient lower crust during the Phanerozoic (Jiang and Guo, 2010; Hu et al., 2020; Zou and Zhang, 2022).

Granulite xenoliths from the NCC were classified into two groups based on their geochemical features in this study. Group I granulite xenoliths are basic-silicic compositions, comprising oligoclase-andesine, almandine-pyrope (Figure 2), augite-diopside and metamorphic ferrosilite (Figures 2 and 3). The Group I granulite xenoliths show relatively lower Mg# values of pyroxenes (Cpx: 54.3–74.6; Opx: 49.8–63.7) and MgO contents of whole rock (0.92–10.9 wt.%) (Figures 3 and 4) than that in the Group II granulite xenoliths and have LREE-enriched patterns (Figure 5) and variable and enriched Sr-Nd isotopic compositions (Figure 6). Their zircon ages vary from the Archean to Phanerozoic, with three peaks of Neoarchean (2.6–2.5 Ga), Paleoproterozoic (1.9–1.8 Ga), and Mesozoic (150–120 Ma) (Figure 7). The Archean zircons show relatively narrow ranges of Hf isotopic compositions, falling into the evolutionary field of the 4.0–2.5 Ga crust (Figure 8). Hf isotopic compositions of some Paleoproterozoic zircons lie within the evolutionary zone of the

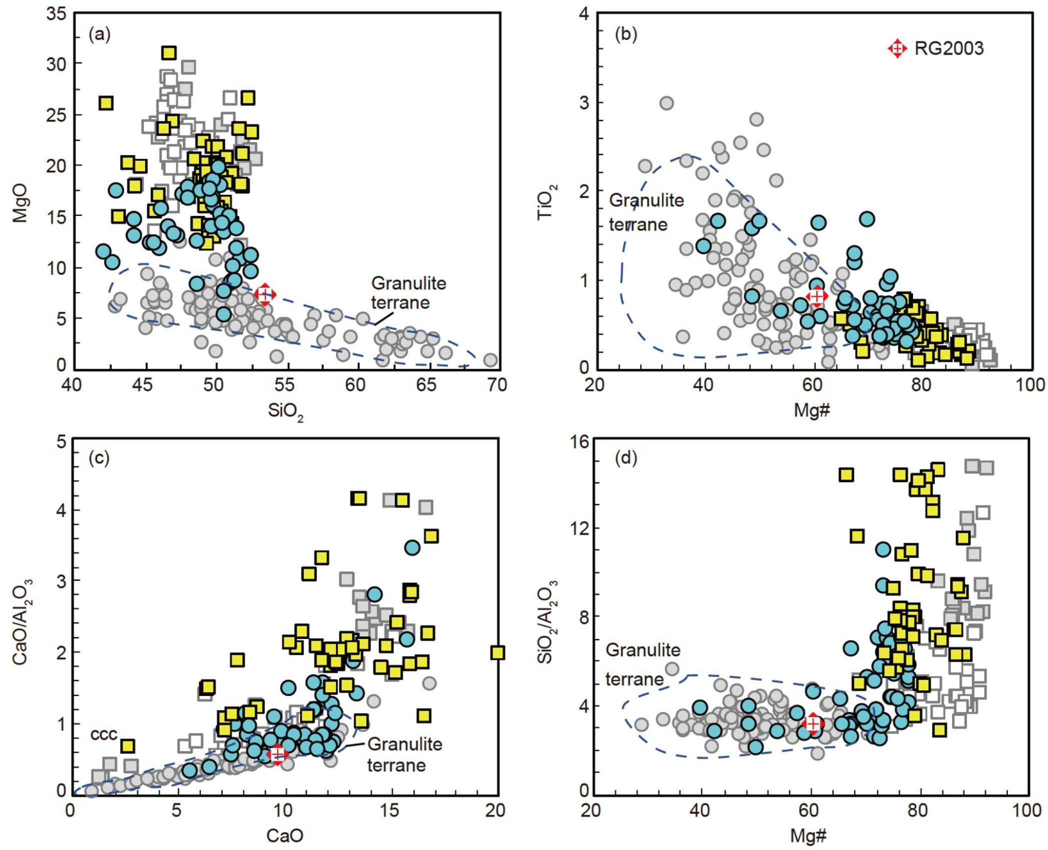

Figure 4 Diagrams of whole-rock major element compositions of granulite and pyroxenite xenoliths. Data sources: granulite xenoliths (Shao and Han, 2000; Liu et al., 2001, 2005, 2010; Zhou et al., 2002; Zheng et al., 2003, 2009a; Huang et al., 2004; Zheng et al., 2004c; He et al., 2009; Jiang et al., 2010, 2011; Ying et al., 2010; Shao and Wei, 2011; Wang et al., 2016; Ma et al., 2017); pyroxenite xenoliths (Liu et al., 2001, 2005, 2020; Xu, 2002; Zheng et al., 2009b; Jiang et al., 2010; Ying et al., 2013b; Hu et al., 2016, 2020; Zhao et al., 2017; Wei et al., 2019; Dai et al., 2021); RG2003 represents compositions of the lower crust calculated by Rudnick and Gao (2014). Data sources of granulite terranes and symbols are the same as Figure 2.

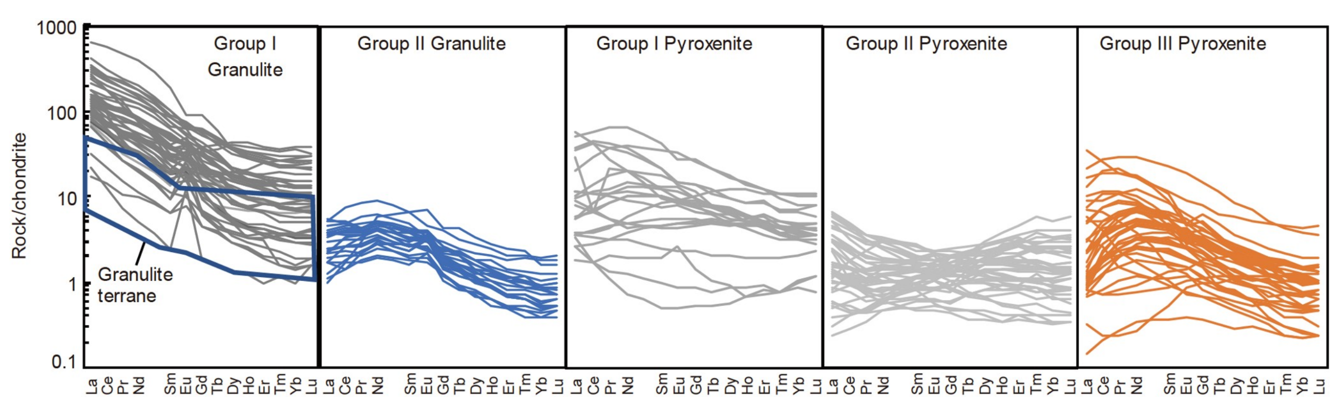

Figure 5 REE patterns of the granulite and pyroxenite xenoliths from the NCC. Chondrite-normalized values are from Sun and McDonough (1989). Other data sources are the same as Figure 4.

Archean crust, while that of others lie near the chondritic values (Figure 8). The Archean-Proterozoic zircons show a large range of oxygen isotopic compositions, with δ^{18}O values from below the mantle value to above the limit of the global Archean-Proterozoic zircons (Figure 8). The Mesozoic zircons have variable Hf isotopic compositions with $\varepsilon_{\mathrm{Hf}}(t)$ values from depleted to enriched, some of which fall into the evolutionary zone of the Archean zircons. The δ^{18}O values of Mesozoic zircons overlap with that of the Archean zircons (Figure 8).

As a whole, the Group I granulite xenoliths show affinities to the NCC granulite terranes in terms of major and trace elements and Sr-Nd isotopic compositions of mineral and whole rock (Figures 2–6). In addition, the Group I granulite

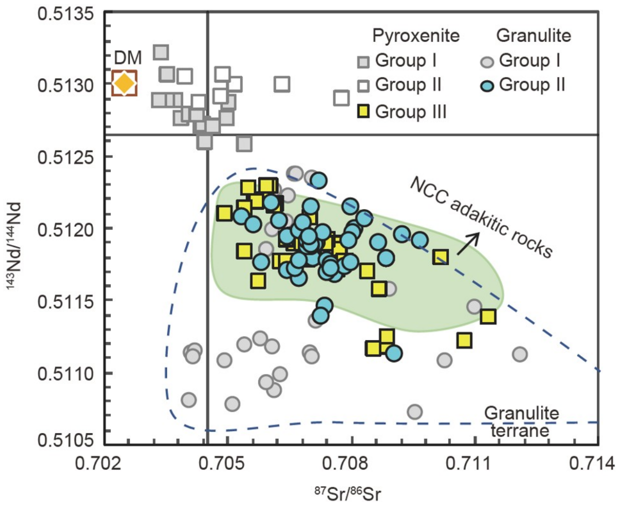

Figure 6 Sr-Nd isotopic compositions of granulite and pyroxenite xenoliths. Data sources: Mesozoic adakitic rocks from the NCC (Zhang et al., 2001c; Xu et al., 2006b; Jiang et al., 2007; Liu S et al., 2009; Chen et al., 2012; Ma et al., 2012, 2015, 2016a, 2016b); depleted mantle (DM) (Zindler and Hart, 1986). Other data sources are the same as Figure 4.

xenoliths have consistent Archean-Paleoproterozoic evolutionary history with the granulite terranes (Figure 7). These observations indicate that the Group I granulite xenoliths could be fragments of the Precambrian lower crust beneath the NCC. Few intermediate granulites in the Group I granulite xenoliths could be restites of partial melting of intermediate-silicic granulites, e.g., those from the Hannuoba and Fuxin regions (Jiang et al., 2009, 2011; Jiang and Guo, 2010; Hu et al., 2020; Zou and Zhang, 2022). Most of the Phanerozoic zircons in the Group I granulite xenoliths are believed to have formed by modification of the older zircons, resulting in the wide ranges of Hf isotopic compositions. Phanerozoic zircons with $\varepsilon_{Hf}(t)$ within the evolution zone of Archean zircons only suffered the resetting of U-Pb ages, whereas those with $\varepsilon_{Hf}(t)$ above the evolution line of Archean zircons reflect the injection of underplated magmas (Zhang et al., 2011; Zhang, 2012). Therefore, we suggest that the Group I granulite xenoliths represent the modified ancient lower crust beneath the NCC.

In contrast, Group II granulite xenoliths are basic compositions and comprise andesine-labradorite-bytownite, pyrope-almandine, augite-diopside (Figure 2), and enstatite-ferrosilite that are magmatic to metamorphic in origin (Figures 2 and 3). Group II granulite xenoliths have higher Mg# values of pyroxenes (Cpx: Mg#=71.8–80.6; Opx: 64.9–79.8) (Figure 3) and MgO contents of whole rock (7.61–19.8 wt.%) (Figure 4) and middle (M)-REE-enriched patterns (Figure 5) than those of Group I granulite xenoliths and granulite terranes. However, the Sr-Nd isotopic compositions of Group II granulite xenoliths fall into the fields of Group I granulite xenoliths and granulite terranes (Figure 6). Zircons in the Group II granulite xenoliths are dominated by Phanerozoic with minor Archean-Proterozoic (Figure 7) and Hf-O isotopic compositions of zircons are similar to that in the Group I granulite xenoliths (Figure 8). These observations indicate that the Group II granulite xenoliths markedly differ from the Precambrian lower crust beneath the NCC. The geochemical features of Group II granulite xenoliths can be explained by the partial melting of the ancient basic lower crust. Partial melting led to an increase in compatible elements, a decrease in incompatible elements in the residues, as manifested by the increased MgO/Mg# and decreased LREE contents in pyroxenes (Figure 3) and whole rock (Figures 4 and 5) of the Group II granulite xenoliths. Few Archean-Proterozoic zircons in the Group II granulite xenoliths could be the results of complete melting or mod-

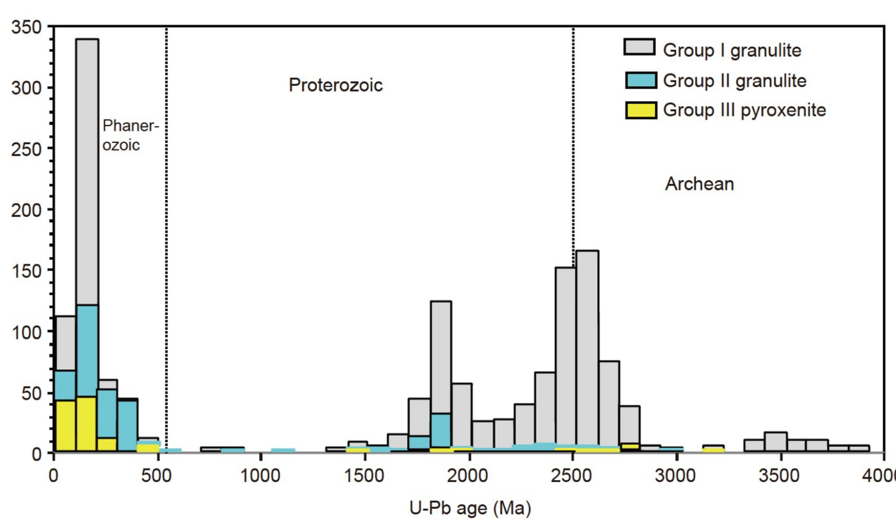

Figure 7 Histogram of zircon U-Pb ages from granulite and pyroxenite xenoliths. Data sources: granulite xenoliths (Liu et al., 2004a, 2010; Zheng et al., 2004b, 2004c, 2009b; Jiang and Guo, 2010; Jiang et al., 2010, 2011; Ying et al., 2010; Zhang, 2012; Wei et al., 2015; Ma et al., 2017, 2020; Ping et al., 2019; Zou et al., 2022); pyroxenite xenoliths (Liu et al., 2004a, 2004b; Zheng et al., 2009b; Jiang et al., 2010; Wei et al., 2015).

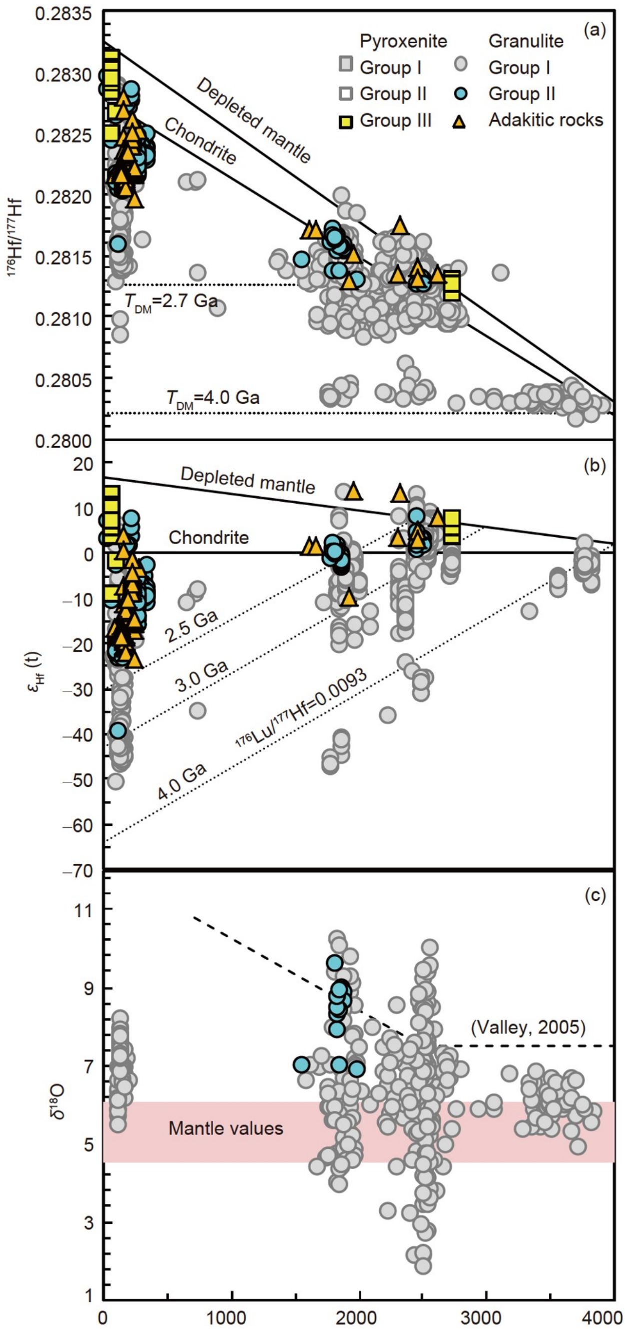

Figure 8 Plots of U-Pb age vs. (a) ^{176}Hf/^{177}Hf ratios (b) $\varepsilon_{Hf}(t)$ and (c) δ^{18}O values in zircons from granulite and pyroxenite xenoliths and Mesozoic adakitic rocks. Data sources: δ^{18}O values of mantle (Valley et al., 2005); Mesozoic adakitic rocks from the NCC (Jiang et al., 2007; Ma and Zheng, 2009; Ma et al., 2012; Ma, 2013); ^{176}Lu/^{177}Hf ratio of crust (Vervoort and Jonathan Patchett, 1996). Other data sources are the same as Figure 7.

ification of the older zircons during the partial melting, as observed in the partial melting experiment of the lower crust that zircons were exhausted at 900°C (Wang, 2020). The negative correlation of Sr and Nd isotopes (Figure 6) and depleted Hf isotopic compositions (Figure 8) of the Phanerozoic zircons of the Group II granulite xenoliths were attributed to the modifications of magma underplating. This is also consistent with previous studies that regarded the Hannuoba basic granulites as residues left after partial melting of ancient basic lower crust (Jiang and Guo, 2010; Hu et al., 2020).

The major and trace elements compositions of Group II granulite xenoliths can also be explained by cumulates formed by mantle-derived magma underplating except the Sr-Nd isotopic compositions. If the Group II granulite xenoliths were formed by magma underplating and contaminated by the ancient lower crust, their Sr-Nd isotopic compositions should change from depleted (e.g., the cumulate Group I pyroxenite) to enriched with the mixing of ancient lower crust. However, such signatures were not observed in the Group II granulite xenoliths, which show enriched Sr-Nd isotopic compositions within the field of Group I granulite xenoliths and granulite terranes (Figure 6). Therefore, the Group II granulite xenoliths are inferred to represent the residues of partial melting of the ancient basic lower crust. Additionally, partial melting experiment of the basic lower crust have proved that the residues could be two-pyroxene granulite and garnet granulite (Springer and Seck, 1997; Qian and Hermann, 2013). The consistent mineral compositions of the experimental residues and the Group II granulite xenoliths (Figures 2 and 3) further support the residual origin of the Group II granulite xenoliths.

4. Lower crustal processes recorded by the pyroxenite xenoliths

Abundant pyroxenite xenoliths also occurred in the Mesozoic-Cenozoic magmatic rocks in the Fangcheng, Junan, Chifeng, Hannuoba, Yangyuan, Sanyitang, Siziwangqi, and Langshan regions of the NCC (Figure 1). Pyroxenite, with variable petrogenesis, could form in the lower crust, crust-mantle transition zones, and lithospheric mantle. Most pyroxenite xenoliths from the NCC were suggested as cumulates from magma underplating in the crust-mantle transition zones, e.g., websterite and garnet pyroxenite xenoliths from the Langshan, Siziwangqi, Yangyuan, Hannuoba, Chifeng, Fuxin, Junan, and Feixian regions (Xu, 2002; Zhang et al., 2007; Ying et al., 2013b; Zou et al., 2014, 2022; Wang et al., 2019; Dai et al., 2021; Liu et al., 2020; Zhao et al., 2021). The Hannuoba garnet pyroxenites and Feixian and Chifeng olivine-websterites were regarded as reaction products of peridotite-silicic melts derived from the recycled lower continental or oceanic crust (Liu et al., 2005; Xu et al., 2013; Zou et al., 2014). However, some Hannuoba websterites were considered to be partial melting residues of ancient basic granulites (Jiang et al., 2010; Hu et al., 2020). Not only dose magma underplating form pyroxenite cumulates directly but also provides heat for the remelting of ancient lower crust. Thus, formation of pyroxenite is vital to understand the evolution of lower crust.

Pyroxenite xenoliths from the NCC were divided into three groups according to their geochemical features in this study. The Group I and II pyroxenite xenoliths are plagioclase-absent websterites and garnet pyroxenites, and have cumulate and reaction origins, respectively. The Group I pyroxenite xenoliths show usually cumulate texture, whereas the Group II pyroxenite xenoliths show reaction texture. Garnets of the Group II pyroxenite xenoliths are pyrope (Figure 2). Clinopyroxene of the Group I and II pyroxenite xenoliths is Mg-rich augite (Figure 2), and orthopyroxene is magmatic enstatite (Figures 2 and 3). Pyroxenes and whole rock of the Group I and II pyroxenite xenoliths have relatively higher Mg# values (Cpx: 83.0–92.7; Opx: 84.5–92.1; whole rock: 75.0–91.9) than those in the granulites and Group III pyroxenite xenoliths (Figures 3 and 4). Group I pyroxenite xenoliths are characterized by LREE- or MREE-enriched patterns, but Group II pyroxenite xenoliths mainly show enrichments in heavy (H)-REE due to the presence of garnets (Figure 5). Moreover, Group I and II pyroxenite xenoliths exhibit depleted Sr-Nd isotopic compositions (Figure 6).

In contrast, the Group III pyroxenite xenoliths comprise andesine-labradorite, pyrope-almandine (Figure 2), augite-diopside, and magmatic to metamorphic orthopyroxenes (Figure 3). Group III pyroxenite xenoliths show relatively lower Mg# values of pyroxenes and whole rocks (Cpx: 74.8–87.8; Opx: 68.3–84.9; whole rock: 66.2–88.1), and enrichments of MREE (Figure 5) and Sr-Nd isotopic compositions (Figure 6) than that in Group I and II pyroxenite xenoliths (Figures 3 and 4). These observations indicate that the Group III pyroxenite xenoliths are not cumulates or reaction products of peridotite-melt but show mineralogical and geochemical affinities to the Group II granulite xenoliths (Figures 2–6). Additionally, zircons of the Group III pyroxenite xenoliths also yielded Archean-Phanerozoic ages with a peak at Mesozoic (Figure 7) and the Phanerozoic zircons have significantly depleted Hf isotopic compositions (Figure 8) similar to those of the Group II granulite xenoliths. This implies that the Group III pyroxenite xenoliths could be as partial melting residues of the ancient basic lower crust as the Group II granulite xenoliths and Hannuoba Al-pyroxenite xenoliths (Jiang et al., 2010; Hu et al., 2020). Furthermore, experimental studies and modal calculations also support that websterite and garnet pyroxenite could be partial melting residues of the basic lower crust (Huang and He, 2010; Qian and Hermann, 2013; Ma et al., 2015). Thus, Group III pyroxenite xenoliths from the NCC represent the reworking products of the ancient basic lower crust, which record directly the transformation processes of the lower crust beneath the NCC.

5. Inversion of the lower crust evolution by adakitic rocks

Apart from the direct records by the lower crust rocks, lower crust-derived magmatic rocks can inverse the evolutionary processes of lower crust. Mesozoic adakitic intermediate-silicic magmatic rocks are widely distributed in the NCC (Figure 1) (Zhang et al., 2003) and generally show high La/Yb and Sr/Y ratios (Zhang et al., 2001a; Liu et al., 2002; Liu S et al., 2009; Xu et al., 2002; Li et al., 2004, 2005; Jiang et al., 2007; Ma et al., 2012, 2016a, 2016b). They were initially considered to originate from the thicker or delaminated lower crust (Zhang et al., 2001a; Gao et al., 2004; Xu et al., 2006b; Xiong et al., 2011). However, recent studies have suggested that the adakitic rocks in the NCC could have been derived from the partial melting of the basic lower crust at medium pressure (10–12.5 kbar), inferring the absence of a thicker lower crust beneath the NCC during the Mesozoic (Xu et al., 2002; Ma et al., 2012, 2015; Qian and Hermann, 2013). Thus, the widespread adakitic rocks in the NCC were products of the partial melting of the basic lower crust. As discussed above, the Group II granulite and Group III pyroxenite xenoliths could be partial melting residues of the ancient basic lower crust. The relationships between the residues and adakitic products need to be ascertained.

Qian and Hermann (2013) conducted an experiment on the partial melting of the basic lower crust from the NCC. The experimental results demonstrated that the generated residues are amphibolite at P=10–15 kbar and T=800°C, the residues are garnet granulite at P=10–12.5 kbar and T=900–1000°C, the residues are two-pyroxene granulite at P=13.5–15 kbar and T=900–1000°C, the residues are garnet pyroxenite at P=15 kbar and T=1050°C, and the residues are websterite at P=10–15 kbar and T=800°C. Moreover, mineral compositions of the experimental residues were in consistent with that of Group II granulite and Group III pyroxenite xenoliths (Figures 2 and 3). We calculated the REE contents of melts and their residues during various degrees partial melting of the ancient basic lower crust represented by the basic Group I granulite xenoliths using the rock-melt partition coefficients (Qian and Hermann, 2013). The results demonstrated significant similarities between the partial melts and adakitic rocks and between the residues and Group II granulite and Group III pyroxenite xenoliths during 30–50% partial melting (Figure 9a–9e). If underplated melts make contributions to the formation of adakitic rocks as suggested by (Chen et al., 2012), 20–30% partial melting of the ancient basic granulites would be better match. The calculated REE patterns of the equilibrium melts with the Group II granulite and Group III pyroxenite xenoliths are consistent with that of the adakitic rocks (Figure 9f). The higher LREE contents in some pyroxenites could be results of late metasomatism. In addition, the adakitic rocks and the

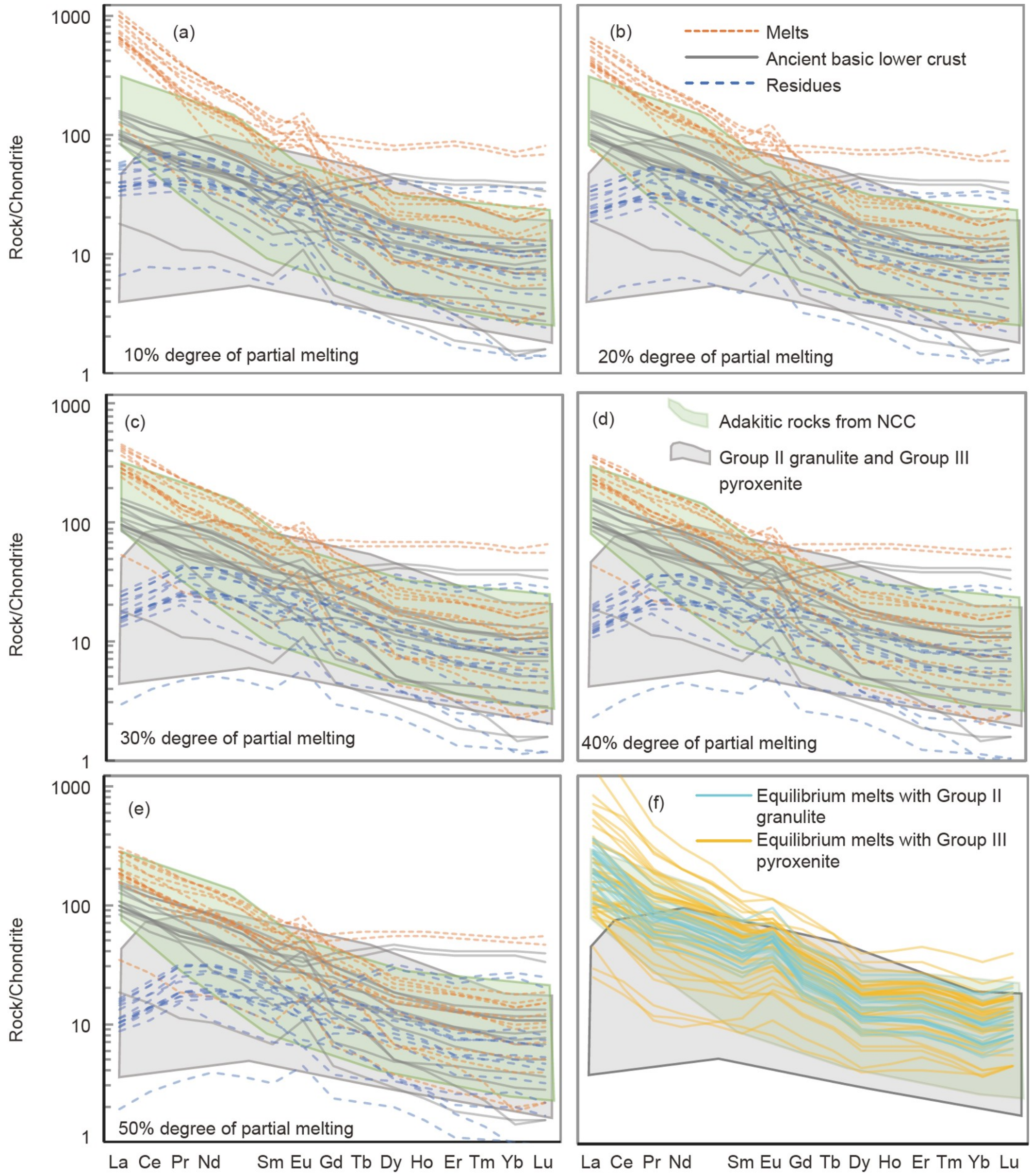

Figure 9 (a)–(e) Calculated REE patterns of partial melts and residues during different degrees of partial melting of ancient basic lower crust and (f) equilibrium melts with the Group II granulite and Group III pyroxenite xenoliths. Data sources: REE partition coefficients of rocks-melt are from Qian and Hermann (2013); adakitic rocks from the NCC (Zhang et al., 2001b; Ma et al., 2015). Ancient basic lower crust was represented by the basic Group I granulite xenoliths and data sources are the same as Figure 4; Chondrite-normalized values sources are the same as Figure 5.

Group II granulite and Group III pyroxenite xenoliths from the NCC show identical Sr-Nd isotopic compositions (Figure 6) (Zhang et al., 2001c; Xu et al., 2006b; Jiang et al., 2007; Liu S et al., 2009; Chen et al., 2012; Ma et al., 2012, 2015, 2016a, 2016b). The Archean-Proterozoic inherited zircons were also found in some Mesozoic adakitic rocks, and the Hf isotopic compositions of all zircons are similar to those of the granulite and pyroxenite xenoliths (Figure 8) (Jiang et al., 2007; Ma and Zheng, 2009; Ma et al., 2012; Ma, 2013). These observations indicate that the adakitic rocks in the NCC are cognate with the residual granulite and pyroxenite xenoliths and the ancient basic lower crust beneath the NCC has experienced extensive partial melting.

6. Evolution and destruction of the lower crust beneath the NCC

Seismological observations have shown that the crust of the NCC gradually thinned from west (~44 km) to east (30–36 km) and exhibited overall intermediate-silicic compositions (Xia et al., 2016). This is generally consistent with the studies on the lower crust xenoliths in the Mesozoic-Cenozoic magmatic rocks, but there are some differences.

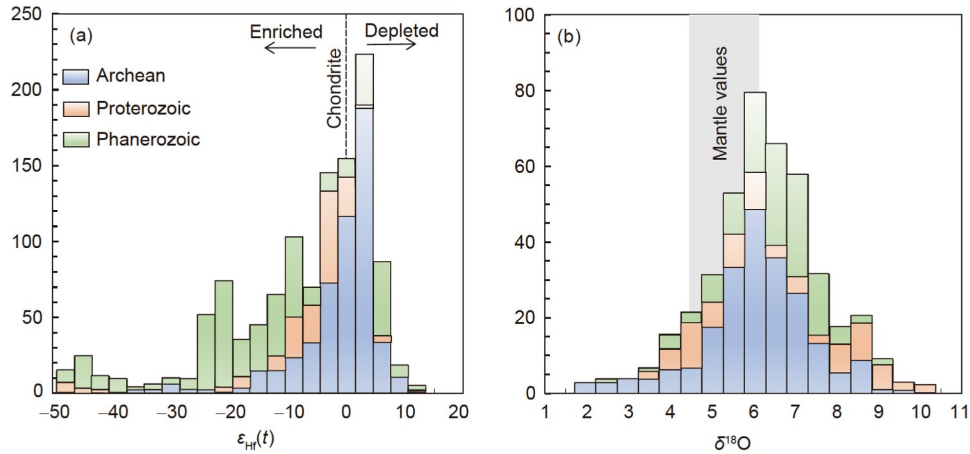

Figure 10 Histogram of $\varepsilon_{Hf}(t)$ and $\delta^{18}O$ values of the Archean, Proterozoic and Phanerozoic zircons. Data sources: mantle $\delta^{18}O$ values (Valley et al., 2005). Other data sources are the same as Figure 7.

For example, the crustal thickness beneath the Xinyang and Xuhuai regions could have been 45 km during the early late-Mesozoic, which could be influenced by the continental collision of the NCC and Yangtze Craton (Li et al., 1993), as evidenced by the identical ages from the lower crust xenoliths and eclogite of the Dabie-Sulu Orogenic Belt. Other granulite xenoliths from the eastern NCC indicate that crustal thickness was <35 km in the Cenozoic, reflecting that the modern crust is thinner than that in the Precambrian (⩾40 km), as constrained by the granulite terranes. The high-density basic lower crust (density >2.9 g cm^{-3}; P-wave velocity=6.8–7.3 km s^{-1}) beneath the NCC in the modern is 4–5 km for the Western Block and <2 km for the Eastern Block and Trans-North China Orogen (Xia et al., 2016), which is generally thinner than that in the Precambrian. These changes could be attributed to the extensive remelting of the ancient basic lower crust during the Phanerozoic, which was transformed into granulite and pyroxenite residues. The P-wave velocities of some basic residues are within the ranges of the crust-mantle transition zones (6.8–7.8 km s^{-1}; Deng and Zhong, 1997) and are clearly different from those of mantle peridotites. However, the P-wave velocities of other residues (e.g., garnet granulite and pyroxenite) are up to 7.8 km s^{-1} (Shao and Han, 2000; Liu et al., 2001; Zheng et al., 2021b), which is close to that of mantle peridotite (7.8–8.2 km s^{-1}). Thus, it is so difficult to distinguish by seismological observations that some residues could be classified as constituents of the upper lithospheric mantle, resulting in the observations of general thin of high density basic lower crust or the crust-mantle transition zones beneath the NCC.

Compared to the granulite terranes, most of granulite and pyroxenite xenoliths from the NCC have abundant Phanerozoic zircons (Figure 7) with positive $\varepsilon_{Hf}(t)$ and near-mantle $\delta^{18}O$ values (Figure 10), suggesting that the ancient lower

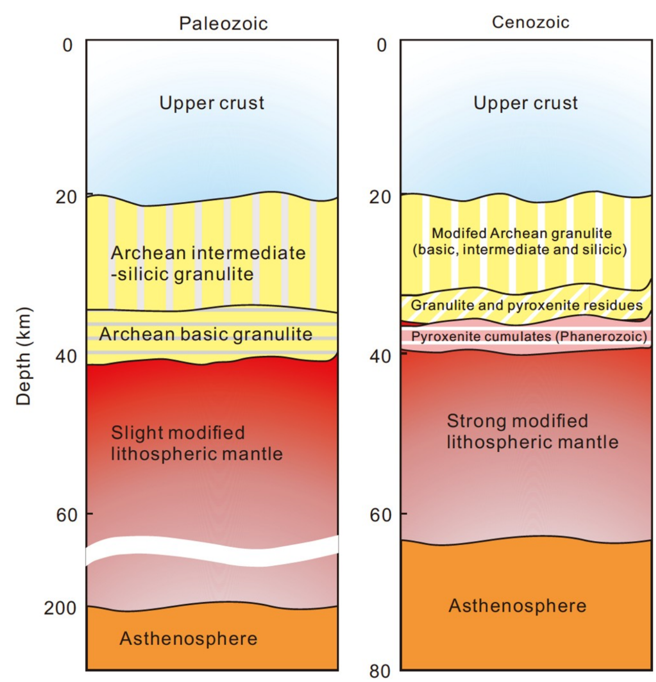

Figure 11 Sketch of lithospheric structure beneath the NCC in the Paleozoic and Cenozoic.

crust was strongly modified by magma underplating. Group I granulite xenoliths with major and trace elements and Sr-Nd isotopic compositions similar to those of the granulite terranes represent the modified ancient lower crust. Group II granulite and Group III pyroxenite xenoliths with higher compatible and lower incompatible elements contents than that of the granulite terranes represent partial melting residues of the ancient basic lower crust. Group I pyroxenite xenoliths are cumulates originated from magma underplating in the crust-mantle transition zones. Consequently, the upper layer of lower crust beneath the eastern NCC is composed of modified ancient granulites, and the lower layer is composed of residues and pyroxenite cumulates (Figure 11). The pyroxenite cumulates provide direct evidence for the extensive magma underplating during the Phanerozoic, which supplied exotic material and heat for the reworking of the ancient lower crust. Additionally, the large-scale lithospheric extension was also one of the reasons for the thinning and melting of the lower crust beneath the NCC (Meng, 2003; Zhai et al., 2003; Wang et al., 2007; Ma and Xu, 2021). Therefore, with extensive magma underplating and lithospheric extension, the lower crust beneath the NCC was continually modified and remelted, resulting in its destruction. The ancient basic lower crust was transformed into granulite and pyroxenite residues and produced adakitic magmatic rocks. Hence, thinning of the lower crust beneath the NCC primarily resulted from the voluminous consumption of ancient lower crust through remelting and some residues (e.g., websterite and garnet granulite) comprise a part of the crust-mantle transition zones. Compositional transformations are mainly due to the injection of underplated magma and partial melting processes.

7. Conclusions

(1) Group I granulite xenoliths show major and trace element and Sr-Nd isotopic compositions and an Archean-Proterozoic evolutionary history similar to that of the granulite terranes. However, they have abundant Phanerozoic zircons with variable Hf isotopic compositions from depleted to enriched, which were formed by modifications of magma underplating. The Group I granulite xenoliths represent modified ancient lower crust beneath the NCC.

(2) Group II granulite and Group III pyroxenite xenoliths have higher MgO and lower incompatible element compositions to those in the granulite terranes and Group I granulite xenoliths, but similar Sr-Nd isotopic compositions and Archean-Phanerozoic evolutionary history to the Group I granulite xenoliths. Their trace element compositions can be complementary with that of the adakitic rocks of the NCC, and Sr-Nd and zircon Hf isotopic compositions are similar to the adakitic rocks. The Group II granulite and Group III pyroxenite xenoliths represent partial melting residues of an ancient basic lower crust that produced voluminous adakitic rocks.

(3) The lower crust beneath the eastern NCC experienced thinning and compositional transformation during the Phanerozoic. Extensive magma underplating not only formed the Group I pyroxenite cumulates in the crust-mantle transition zones during the Mesozoic-Cenozoic, but also provided exotic materials and heat for the modifications and remelting of the ancient lower crust. These processes resulted in the destruction of lower crust beneath the NCC.

Acknowledgements *We sincerely appreciate the constructive and beneficial suggestions from Editorial Board members and two anonymous reviewers. This work was supported by the National Natural Science Foundation of China (Grant Nos. 41688103 & 42003026).*

References

Bhattacharyya C. 1971. An evaluation of the chemical distinctions between igneous and metamorphic orthopyroxenes. Amer Mineral, 56: 499–506

Chen B, Jahn B M, Suzuki K. 2012. Petrological and Nd-Sr-Os isotopic constraints on the origin of high-Mg adakitic rocks from the North China Craton: Tectonic implications. Geology, 41: 91–94

Chen S H, O'Reilly S Y, Zhou X H, Griffin W L, Zhang G H, Sun M, Feng J L, Zhang M. 2001. Thermal and petrological structure of the lithosphere beneath Hannuoba, Sino-Korean Craton, China: Evidence from xenoliths. Lithos, 56: 267–301

Cui W Y, Wang C Q. 1992. Evolution of metamorphism of Archean Jianping metamorphic complex from the Western Liaoning Province. Acta Sci Natural, 28: 745–759

Cui W Y, Wang C Q, Wang S Q. 1991. Geochemistry and metamorphism *P-T-t* path of the Archean Jianping metamorphic complex in Western Liaoning province (in Chinese with English abstract). Acta Petrol Sin, 4: 13–27

Dai H K, Zheng J P, Griffin W L, O'Reilly S Y, Xiong Q, Ping X Q, Chen F K, Lu J G. 2021. Pyroxenite xenoliths record complex melt impregnation in the deep lithosphere of the Northwestern North China Craton. J Petrol, 62: egaa079

Deng J F, Su S G, Liu C, Zhao G C, Zhao X G, Zhou S, Wu Z X. 2006. Discussion on the lithospheric thinning of the North China Craton: Delamination? or therm erosion and chemical metamosatism? (in Chines with English abstract) Earth Sci Front, 13: 105–119

Deng W M, Zhong D L. 1997. Crust-mantle transition and its geological meaning in the lithsopheric evolution (in Chinese). Chin Sci Bull, 42: 2474–2482

Du X X, Fan Q C. 2011. Discussion on genesis of pyroxenite and granulite xenoliths from Hannuoba (in Chinese with English abstract). Acta Petrol Sin, 27: 2927–2936

Fan Q C, Liu R X. 1996. High-temperature granulite xenoliths in Hannuoba basalt (in Chinese). Chin Sci Bull, 41: 235–238

Fan W M, Zhang H F, Baker J, Jarvis K E, Mason P R D, Menzies M A. 2000. On and off the North China Craton: Where is the Archaean keel? J Petrol, 41: 933–950

Gao S, Rudnick R L, Yuan H L, Liu X M, Liu Y S, Xu W L, Ling W L, Ayers J, Wang X C, Wang Q H. 2004. Recycling lower continental crust in the North China Craton. Nature, 432: 892–897

Griffin W, Zhang A, O'Reilly S, Ryan C. 1998. Phanerozoic evolution of the lithosphere beneath the Sino-Korean Craton. Mantle Dynamics and Plate Interactions in East Asia 27: 107–126

Guo J H, Sun M, Chen F K, Zhai M G. 2005. Sm-Nd and SHRIMP U-Pb zircon geochronology of high-pressure granulites in the Sanggan area, North China Craton: Timing of Paleoproterozoic continental collision. J Asian Earth Sci, 24: 629–642

Guo J H, Zhai M G. 2000. Sm-Nd age dating of high-pressure granulites and amphibolite from Sanggan area, North China Craton. Chin Sci Bull, 46: 106–111

Guo J H, Zhai M G, Li Y, Yan Y. 1998. Contrasting metamorphic *P-T* paths of Archean high-pressure granulites from the North China Craton: Metamorphism and tectonic significance (in Chinese with English abstract). Acta Petrol Sin, 14: 430–448

Guo J H, Zhai M G, Xu R H. 2001. Timing of the granulite facies metamorphism in the Sanggan area, North China Craton: Zircon U-Pb geochronology. Sci China Ser D-Earth Sci, 44: 1010–1018

He Y K, Wu T R, Jing X, Luo H L, Zhao L. 2009. Early Cretaceous underplating of the northern margin of North China Craton: Evidence from the granulite xenoliths (in Chinese with English Abstract). Acta Petrol Sin, 25: 1201–1215

Hu J, Jiang N, Guo J H, Fan W B, Liu D Q. 2020. The role of basaltic underplating in the evolution of the lower continental crust. Geochim Cosmochim Acta, 275: 19–35

Hu Y, Teng F Z, Zhang H F, Xiao Y, Su B X. 2016. Metasomatism-induced mantle magnesium isotopic heterogeneity: Evidence from pyroxenites. Geochim Cosmochim Acta, 185: 88–111

Huang F, He Y S. 2010. Partial melting of the dry mafic continental crust: Implications for petrogenesis of C-type adakites (in Chinese). Chin Sci Bull, 55: 1255–1267

Huang X L, Xu Y G, Chu X L, Zhang H X, Liu C Q. 2001. Geochemical comparative studies of some granulite terrains and granulite xenoliths from North China Craton (in Chinese with English abstract). Acta Petrol Mineral, 20: 318–328

Huang X L, Xu Y G, Liu D Y. 2004. Geochronology, petrology and geochemistry of the granulite xenoliths from Nushan, east China: Implication for a heterogeneous lower crust beneath the Sino-Korean Craton. Geochim Cosmochim Acta, 68: 127–149

Jiang N, Carlson R, Guo J H. 2011. Source of Mesozoic intermediate-felsic igneous rocks in the North China Craton: Granulite xenolith evidence. Lithos, 125: 335–346

Jiang N, Guo J H. 2010. Hannuoba intermediate-mafic granulite xenoliths revisited: Assessment of a Mesozoic underplating model. Earth Planet Sci Lett, 293: 277–288

Jiang N, Guo J H, Zhai M G, Zhang S Q. 2010. ~2.7 Ga crust growth in the North China Craton. Precambrian Res, 179: 37–49

Jiang N, Liu Y S, Zhou W G, Yang J H, Zhang S Q. 2007. Derivation of Mesozoic adakitic magmas from ancient lower crust in the North China Craton. Geochim Cosmochim Acta, 71: 2591–2608

Jiang N, Zhang S Q, Wen G Z, Liu Y S. 2009. Origin of a Mesozoic granite with A-type characteristics from the North China Craton: Highly fractionated from I-type magmas? Contrib Mineral Petrol, 158: 113–130

Jin S Q, Li D C. 1986. Pyroxene from granulite-facies metamorphic rocks, North China (in Chinese). Bull Changchun Geol, 16: 29–36

Li C D, Zhang Q, Miao L C, Meng X F. 2004. Mesozoic high-Sr, low-Y and low-Sr, low-Y types granitoids in the northern Hebei province: Geochemistry and petrogenesis and its relation to mineralization of gold deposits (in Chinese with English abstract). Acta Petrol Sin, 20: 269–284

Li S G, Wang Y. 2018. Formation time of the big mantle wedge beneath eastern China and a new lithospheric thinning mechanism of the North China Craton—Geodynamic effects of deep recycled carbon. Sci China Earth Sci, 61: 853–868

Li S G, Xiao Y L, Liou D, Chen Y Z, Ge N J, Zhang Z Q, Sun S S, Cong B L, Zhang R Y, Hart S R, Wang S S. 1993. Collision of the North China and Yangtse Blocks and formation of coesite-bearing eclogites: Timing and processes. Chem Geol, 109: 89–111

Li W P, Li X H, Lu F X. 2005. Genesis and geological significance for the middle Jurassic high Sr and low Y type volcanic rocks in Fuxin area of west Liaoning, northeastern China (in Chinese with English abstract). Acta Petrol Sin, 17: 523–532

Liu F L. 1997. The metamorphic reaction and water activity of basic granulite in the Datong-Huaian Region (in Chinese with English abstract). Acta Petrol Sin, 13: 33–42

Liu H T, Sun S H, Liu J M, Zhai M G. 2002. The Mesozoic high-Sr granitoids in the northern marginal region of North China Craton: Geochemistry and source region (in Chinese with English abstract). Acta Petrol Sin, 18: 18–29

Liu S, Hu R Z, Gao S, Feng C X, Yu B B, Qi Y Q, Wang T, Feng G Y, Coulson I M. 2009. Zircon U-Pb age, geochemistry and Sr-Nd-Pb isotopic compositions of adakitic volcanic rocks from Jiaodong, Shandong Province, Eastern China: Constraints on petrogenesis and implications. J Asian Earth Sci, 35: 445–458

Liu Y C, Wang A D, Rolfo F, Groppo C, Gu X F, Song B. 2009. Geochronological and petrological constraints on Palaeoproterozoic granulite facies metamorphism in southeastern margin of the North China Craton. J Metamorph Geol, 27: 125–138

Liu Y D, Ying J F, Li J, Sun Y, Teng F Z. 2020. Diverse origins of pyroxenite xenoliths from Yangyuan, North China Craton: Implications for the modification of lithosphere by magma underplating and melt-rock interactions. Lithos, 372-373: 105680

Liu Y S, Gao S, Gao C G, Zong K Q, Hu Z C, Ling W L. 2010. Garnet-rich granulite xenoliths from the Hannuoba Basalts, North China: Petrogenesis and implications for the Mesozoic crust-mantle interaction. J Earth Sci, 21: 669–691

Liu Y S, Gao S, Jin S Y, Hu S H, Sun M, Zhao Z B, Feng J L. 2001. Geochemistry of lower crustal xenoliths from Neogene Hannuoba basalt, North China Craton: Implications for petrogenesis and lower crustal composition. Geochim Cosmochim Acta, 65: 2589–2604

Liu Y S, Gao S, Lee C T A, Hu S H, Liu X M, Yuan H L. 2005. Melt–peridotite interactions: Links between garnet pyroxenite and high-Mg# signature of continental crust. Earth Planet Sci Lett, 234: 39–57

Liu Y S, Gao S, Liu X M, Chen X M, Zhang W L, Wang X C. 2003. Lithospheric thermal dynamic reorded by lower crust-upper mantle xenolith from Hannuoba (in Chinese). Chin Sci Bull, 48: 1575–1581

Liu Y S, Gao S, Yuan H L, Zhou L, Liu X M, Wang X C, Hu Z C, Wang L S. 2004a. U-Pb zircon ages and Nd, Sr, and Pb isotopes of lower crustal xenoliths from North China Craton: Insights on evolution of lower continental crust. Chem Geol, 211: 87–109

Liu Y S, Yuan H L, Gao S, Hu Z C, Wang X C, Liu X M, Ling W L. 2004b. Zircon U-Pb ages from Hannuoba olivine-pyroxenite xenolith: Relations between 97–158 Ma magma underplating and granulite metamorphism (in Chinese). Chin Sci Bull, 49: 790–797

Lu H S, Wei C J. 2020. Late Neoarchean or late Paleoproterozoic high-pressure granulite facies metamorphism from the East Hebei terrane, North China Craton? J Asian Earth Sci, 190: 104195

Ma Q. 2013. Triassic-Jurassic Volcanic Rocks in Western Liaoning: Implications for Lower Crustal Reworking and Lithospheric Destruction in the North Part of Eastern North China Craton (in Chinese). Doctoral Dissertation. Wuhan: Chinese University of Geoscience

Ma Q, Xu Y G. 2021. Magmatic perspective on subduction of Paleo-Pacific plate and initiation of big mantle wedge in East Asia. Earth-Sci Rev, 213: 103473

Ma Q, Xu Y G, Huang X L, Zheng J P, Ping X, Xia X P. 2020. Eoarchean to Paleoproterozoic crustal evolution in the North China Craton: Evidence from U-Pb and Hf-O isotopes of zircons from deep-crustal xenoliths. Geochim Cosmochim Acta, 278: 94–109

Ma Q, Xu Y G, Zheng J P, Griffin W L, Hong L B, Ma L. 2016a. Coexisting Early Cretaceous high-Mg andesites and adakitic rocks in the North China Craton: The role of water in intraplate magmatism and cratonic destruction. J Petrol, 57: 1279–1308

Ma Q, Xu Y G, Zheng J P, Sun M, Griffin W L, Xia X, Pan S K. 2017. Phanerozoic magma underplating and crustal growth beneath the North China Craton. Terra Nova, 29: 211–217

Ma Q, Xu Y G, Zheng J P, Sun M, Griffin W L, Wei Y, Ma L, Yu X. 2016b. High-Mg adakitic rocks and their complementary cumulates formed by crystal fractionation of hydrous mafic magmas in a continental crustal magma chamber. Lithos, 260: 211–224

Ma Q, Zheng J P. 2009. *In-situ* U-Pb dating and Hf isotopic analyses of zircons in the volcanic rock of the Lanqi Formation in the Beipiao area, Western Liaoning Province (in Chinese with English abstract). Acta Geol Sin, 25: 3287–3297

Ma Q, Zheng J P, Griffin W L, Zhang M, Ping X Q. 2012. Triassic "adakitic" rocks in an extensional setting (North China): Melts from the cratonic lower crust. Lithos, 149: 159–173

Ma Q, Zheng J P, Xu Y G, Griffin W L, Zhang R S. 2015. Are continental "adakites" derived from thickened or foundered lower crust? Earth Planet Sci Lett, 419: 125–133

Meng Q R. 2003. What drove late Mesozoic extension of the northern China–Mongolia tract? Tectonophysics, 369: 155–174

Menzies M A, Fan W, Zhang M. 1993. Palaeozoic and Cenozoic lithoprobes and the loss of >120 km of Archaean lithosphere, Sino-Korean craton, China. J Geol Soc, 76: 71–81

Ping X Q, Zheng J P, Tang H Y, Xiong Q, Su Y P. 2015. Paleoproterozoic multistage evolution of the lower crust beneath the southern North

China Craton. Precambrian Res, 269: 162–182
Ping X Q, Zheng J P, Xiong Q, Griffin W L, Yu C M, Su Y P. 2019. Downward rejuvenation of the continental lower crust beneath the southeastern North China Craton. Tectonophysics, 750: 213–228
Qian Q, Hermann J. 2013. Partial melting of lower crust at 10–15 kbar: Constraints on adakite and TTG formation. Contrib Mineral Petrol, 165: 1195–1224
Rietmeijer F J M. 1983. Chemical distinction between igneous and metamorphic orthopyroxenes especially those coexisting with Ca-rich clinopyroxenes: A re-evaluation. Mineral mag, 47: 143–151
Rudnick R L, Gao S. 2014. 4.1–composition of the continental crust. In: Holland H D, Turekian K K, eds. Treatise on Geochemistry. 2nd ed. Oxford: Elsevier. 1–51
Shao J A, Han Q J. 2000. Early Mesozoic mantle-crust transitional zone in eastern Inner Mongolia: Evidence from measurements of compressional velocities of xenoliths at high pressure and high temperature. Sci China Ser D-Earth Sci, 43: 253–261
Shao J A, Wei C J. 2011. Petrology and tectonic significance of the early Mesozoic granulite xenoliths from the eastern Inner Mongolia, China. Sci China Earth Sci, 54: 1484–1491
Shao J A, Zhang Z, She H Q. 2012. The discovery of Phanerozoic granulite in Chifeng are of North Craton and its implication (in Chinese with English abstract). Earth Sci Front, 19: 188–198
Springer W, Seck H A. 1997. Partial fusion of basic granulites at 5 to 15 kbar: Implications for the origin of TTG magmas. Contrib Mineral Petrol, 127: 30–45
Sun S S, McDonough W F. 1989. Chemical and isotopic systematics of oceanic basalts: Implications for mantle composition and processes. Geol Soc London Spec Publ, 42: 313–345
Tang Y J, Ying J F, Zhao Y P, Xu X R. 2021. Nature and secular evolution of the lithospheric mantle beneath the North China Craton. Sci China Earth Sci, 64: 1492–1503
Valley J, Lackey J, Cavosie A, Clechenko C, Spicuzza M, Basei M, Bindeman I, Ferreira V, Sial A, King E, Peck W, Sinha A, Wei C. 2005. 4.4 billion years of crustal maturation: Oxygen isotope ratios of magmatic zircon. Contrib Mineral Petrol, 150: 561–580
Vervoort J D, Jonathan Patchett P. 1996. Behavior of hafnium and neodymium isotopes in the crust: Constraints from Precambrian crustally derived granites. Geochim Cosmochim Acta, 60: 3717–3733
Wang C, Liu Y, Foley S F, Zong K, Hu Z. 2019. Lithospheric transformation of the northern North China Craton by changing subduction style of the Paleo-Asian oceanic plate: Constraints from peridotite and pyroxenite xenoliths in the Yangyuan basalts. Lithos, 328-329: 58–68
Wang K, Zhao L, Xu X B, Yang J F. 2018. Heterogeneous destruction of the North China Craton: Coupled constraints from seismology and geodynamic numerical modeling. Sci China Earth Sci, 61: 515–526
Wang T, Zheng Y D, Zhang J J, Wang X S, Zeng L S, Tong Y. 2007. Some problems in the study of Mesozoic extensional structure in the North China Craton and its significance for the study of lithospheric thinning (in Chinese with English abstract). Geol Bull Chin, 26: 1154–1166
Wang X. 2020. Investigation on the Rheology and partial melting of garnet amphibolites of the lower crust of the Tibetan Plateau (in Chinese). Doctoral Dissertation. Wuhan: China University of Geosciences
Wang Y, Sun L X, Zhou L Y, Xie Y T. 2018. Discussion on the relationship between the Yanshanian Movement and cratonic destruction in North China. Sci China Earth Sci, 61: 499–514
Wang Z Z, Liu S A, Ke S, Liu Y C, Li S G. 2016. Magnesium isotopic heterogeneity across the cratonic lithosphere in eastern China and its origins. Earth Planet Sci Lett, 451: 77–88
Wei C J. 2018. Neoarchean granulite facies metamorphisam and its tectonic implications from the East Hebei terrane (in Chinese with English abstract). Acta Petrol Sin, 34: 895–912
Wei Y, Mukasa S B, Zheng J, Fahnestock M F, Bryce J G. 2019. Phanerozoic lower crustal growth from heterogeneous mantle beneath the North China Craton: Insights from the diverse Hannuoba pyroxenite xenoliths. Lithos, 324-325: 55–67
Wei Y, Zheng J P, Su Y P, Ma Q, Griffin W L. 2015. Lithological and age structure of the lower crust beneath the northern edge of the North China Craton: Xenolith evidence. Lithos, 216-217: 211–223
Wu F Y, Xu Y G, Zhu R X, Zhang G W. 2014. Thinning and destruction of the cratonic lithosphere: A global perspective. Sci China Earth Sci, 57: 2878–2890
Xia B, Thybo H, Artemieva I M. 2016. Seismic crustal structure of the North China Craton and surrounding area: Synthesis and analysis. J Geophys Res-Solid Earth, 122: 5181–5207
Xiong X L, Liu X C, Zhu Z M, Li Y, Xiao W S, Song M S, Zhang S, Wu J H. 2011. Adakitic rocks and destruction of the North China Craton: Evidence from experimental petrology and geochemistry. Sci China Earth Sci, 54: 858–870
Xu J F, Shinjo R, Defant M J, Wang Q, Rapp R P. 2002. Origin of Mesozoic adakitic intrusive rocks in the Ningzhen area of east China: Partial melting of delaminated lower continental crust? Geology, 30: 1111
Xu N Q, Zhao G C, Zhang H C G, Wang C, Yao J L. 2021. Phase equilibria modelling and zircon U-Pb ages of the Paleoproterozoic high-pressure mafic granulites in the Jianping Complex and tectonic implications. Precambrian Res, 367: 106460
Xu W L, Gao S, Wang Q H, Wang D Y, Liu Y S. 2006a. Mesozoic crustal thickening of the eastern North China Craton: Evidence from eclogite xenoliths and petrologic implications. Geology, 34: 721
Xu W L, Wang Q H, Wang D Y, Guo J H, Pei F P. 2006b. Mesozoic adakitic rocks from the Xuzhou-Suzhou area, eastern China: Evidence for partial melting of delaminated lower continental crust. J Asian Earth Sci, 27: 454–464
Xu W L, Zhou Q J, Pei F P, Yang D B, Gao S, Li Q L, Yang Y H. 2013. Destruction of the North China Craton: Delamination or thermal/chemical erosion? Mineral chemistry and oxygen isotope insights from websterite xenoliths. Gondwana Res, 23: 119–129
Xu Y G. 2002. Evidence for crustal components in the mantle and constraints on crustal recycling mechanisms: Pyroxenite xenoliths from Hannuoba, North China. Chem Geol, 182: 301–322
Yang C, Wei C J. 2017. Two phases of granulite facies metamorphism during the Neoarchean and Paleoproterozoic in the East Hebei, North China Craton: Records from mafic granulites. Precambrian Res, 301: 49–64
Ying J F, Zhang H F, Tang Y J. 2010. Lower crustal xenoliths from Junan, Shandong province and their bearing on the nature of the lower crust beneath the North China Craton. Lithos, 119: 363–376
Ying J F, Zhang H F, Tang Y J. 2013a. Phanerozoic modification of the lower crust beneath the North China Craton: Constraints from granulite xenoliths (in Chinese with English abstract). Acta Petrol Mineral, 32: 567–576
Ying J F, Zhang H F, Tang Y J, Su B X, Zhou X H. 2013b. Diverse crustal components in pyroxenite xenoliths from Junan, Sulu orogenic belt: Implications for lithospheric modification invoked by continental subduction. Chem Geol, 356: 181–192
Zhai M G. 2004. Precambrian tectonic evolution of the North China Craton. SP, 226: 57–72
Zhai M G. 2008. Lower crust and lithsopheric mantle beneath the North China Craton before the Mesozoic lithospheric disruption (in Chinese with English abstract). Acta Petrol Sin, 24: 2185–2204
Zhai M G. 2009. Two kinds of granulites (HT-HP and HT-UHT) in North China Craton: Their genetic relation ans geotectonic implications (in Chinese with English abstract). Acta Petrol Sin, 25: 1753–1771
Zhai M G, Fan Q C, Zhang H F, Sui J L, Shao J A. 2007. Lower crustal processes leading to Mesozoic lithospheric thinning beneath eastern North China: Underplating, replacement and delamination. Lithos, 96: 36–54
Zhai M G, Guo J H. 1992. Discovery and the implication for the deep crust of high-pressure basic granulite from the North China. Adv Earth Sci, 7: 60–63
Zhai M G, Liu W J. 2001. The formation of granulite and its contribution to evolution of the continental crust (in Chinese with English abstract).

Acta Petrol Sin, 17: 28–38
Zhai M G, Zhu R X, Liu J M, Meng Q R, Hou Q L, Hu S B, Li Z J, Zhang H F. 2003. Mesozoic tectonic system transition of the eastern North China. Sci China Ser D-Earth Sci, 33: 961–969
Zhang H F. 2009. Peridotite-melt interaction: A key point for the destruction of cratonic lithospheric mantle (in Chinese). Chin Sci Bull, 54: 3417–3437
Zhang H F. 2012. Destruction of ancient lower crust through magma underplating beneath Jiaodong Peninsula, North China Craton: U-Pb and Hf isotopic evidence from granulite xenoliths. Gondwana Res, 21: 281–292
Zhang H F, Ying J F, Shimoda G, Kita N T, Morishita Y, Shao J A, Tang Y J. 2007. Importance of melt circulation and crust-mantle interaction in the lithospheric evolution beneath the North China Craton: Evidence from Mesozoic basalt-borne clinopyroxene xenocrysts and pyroxenite xenoliths. Lithos, 96: 67–89
Zhang H F, Ying J F, Tang Y J, Li X H, Feng C, Santosh M. 2011. Phanerozoic reactivation of the Archean North China Craton through episodic magmatism: Evidence from zircon U-Pb geochronology and Hf isotopes from the Liaodong Peninsula. Gondwana Res, 19: 446–459
Zhang J, Zhang H F. 2007. Composition features and *P*-*T* conditions of granulite xenoliths from late Cretaceous mafic dike, Qingdao region (in Chinese with English abstract). Acta Petrol Sin, 23: 1133–1140
Zhang Q, Qian Q, Wang E, Wang Y, Zhao T P, Hao J, Guo G J. 2001a. An east China plateau in mid-late Yanshanian period: Implication from adakities (in Chinese with English abstract). Chin J Geol, 36: 248–255
Zhang Q, Wang Y, Liu H T, Wang Y L, Li Z T. 2003. On the space-time distribution and geodynamic environments of adakites in China annex: Controversies over differing opinions for adakites in China (in Chinese with English absract). Earth Sci Front, 4: 385–400
Zhang Q, Wang Y, Qian Q, Yang J H, Wang Y L, Zhao T P, Guo G J. 2001b. The characteristics and tectonic-metallogenic significances of the adakites in Yanshan period from eastern China (in Chinese with English abstract). Acta Petrol Sin, 17: 236–244
Zhang Q, Wang Y, Wang Y L. 2001c. Preliminary study on the components of the lower crust in east China Plateau during Yanshanian Period: Constraints on Sr and Nd isotopic compositions of adakite-like rocks (in Chinese with English abstract). Acta Petrol Sin, 17: 505–513
Zhang R Y, Cong B L, Ying Y P. 1982. The studies of pyroxene in granulite from Taipingzhai region, eastern Hebei province (in Chinese with English abstract). Chin J Geol, 17: 134–143
Zhang Y L, Zhang H F, Bao Z A, Santosh M, Yuan H L. 2016. Heterogeneous Pb isotope composition in the Archean lower crust of the North China Craton induced by Cenozoic basaltic magma underplating. J Asian Earth Sci, 125: 71–86
Zhao G, Cawood P A, Li S, Wilde S A, Sun M, Zhang J, He Y, Yin C. 2012. Amalgamation of the North China Craton: Key issues and discussion. Precambrian Res, 222-223: 55–76
Zhao G C, Sun M, Wilde S, Li S Z. 2005. Archean to Paleoproterozoic evolution of the North China Craton. J Asian Earth Sci, 24: 519–522
Zhao X M, Cao H, Mi X, Evans N, Qi Y, Huang F, Zhang H. 2017. Combined iron and magnesium isotope geochemistry of pyroxenite xenoliths from Hannuoba, North China Craton: Implications for mantle metasomatism. Contrib Mineral Petrol, 172: 40
Zhao X M, Wang H, Li Z H, Evans N J, Ying J F, Yang Y H, Zhang H F. 2021. Nature and evolution of lithospheric mantle beneath the western North China Craton: Constraints from peridotite and pyroxenite xenoliths in the Sanyitang basalts. Lithos, 384-385: 105987
Zheng J P, Griffin W L, Ma Q, O'Reilly S Y, Xiong Q, Tang H Y, Zhao J H, Yu C M, Su Y P. 2012. Accretion and reworking beneath the North China Craton. Lithos, 149: 61–78
Zheng J P, Griffin W, O'Reilly S, Lu F X, Wang C Y, Zhang M, Wang F Z, Li H M. 2004a. 3.6 Ga lower crust in central China: New evidence on the assembly of the North China Craton. Geology, 32: 229
Zheng J P, Griffin W, O'Reilly S, Lu F X, Yu C M, Zhang M, Li H M. 2004b. U-Pb and Hf-isotope analysis of zircons in mafic xenoliths from Fuxian kimberlites: Evolution of the lower crust beneath the North China Craton. Contrib Mineral Petrol, 148: 79–103
Zheng J P, Griffin W L, O'Reilly S Y, Zhao J H, Wu Y B, Liu G L, Pearson N, Zhang M, Ma C Q, Zhang Z H, Yu C M, Su Y P, Tang H Y. 2009a. Neoarchean (2.7–2.8 Ga) accretion beneath the North China Craton: U-Pb age, trace elements and Hf isotopes of zircons in diamondiferous kimberlites. Lithos, 112: 188–202
Zheng J P, Griffin W L, Qi L, O'Reilly S Y, Sun M, Zheng S, Pearson N, Gao J F, Yu C M, Su Y P, Tang H Y, Liu Q S, Wu X L. 2009b. Age and composition of granulite and pyroxenite xenoliths in Hannuoba basalts reflect Paleogene underplating beneath the North China Craton. Chem Geol, 264: 266–280
Zheng J P, Sun M, Lu F X, Pearson N. 2003. Mesozoic lower crustal xenoliths and their significance in lithospheric evolution beneath the Sino-Korean Craton. Tectonophysics, 361: 37–60
Zheng J P, Xia B, Dai H K, Ma Q. 2021a. Lithospheric structure and evolution of the North China Craton: An integrated study of geophysical and xenolith data. Sci China Earth Sci, 64: 205–219
Zheng J P, Xia B, Ping X Q, Wei Y, Tang H Y, Su Y P, Ma Q. 2021b. Rock probes and seismic methods to constrain the structure, composition and evolution of the deep crust beneath North China Block. Chin Sci Bull, 66: 3018–3031
Zheng J P, Yu C M, Lu F X, Li H M. 2004c. Zircon geochronology and geochemistry of mafic xenoliths from Liaoning kimberlites: Track the early evolution of the lower crust, North China Craton. Sci China Ser D-Earth Sci, 47: 961–972
Zheng Y F, Xu Z, Zhao Z F, Dai L Q. 2018. Mesozoic mafic magmatism in North China: Implications for thinning and destruction of cratonic lithosphere. Sci China Earth Sci, 61: 353–385
Zhou X H, Sun M, Zhang G, Chen S. 2002. Continental crust and lithospheric mantle interaction beneath North China: Isotopic evidence from granulite xenoliths in Hannuoba, Sino-Korean craton. Lithos, 62: 111–124
Zhu R X, Xu Y G. 2019. The subduction of the west Pacific plate and the destruction of the North China Craton. Sci China Earth Sci, 62: 1340–1350
Zindler A, Hart S. 1986. Chemical Geodynamics. Annu Rev Earth Planet Sci, 14: 493–571
Zong K Q, Liu Y S. 2018. Carbonate metasomatism in the lithospheric mantle: Implications for cratonic destruction in North China. Sci China Earth Sci, 61: 711–729
Zou D Y, Liu Y S, Hu Z C, Gao S, Zong K Q, Xu R, Deng L X, He D T, Gao C G. 2014. Pyroxenite and peridotite xenoliths from Hexigten, Inner Mongolia: Insights into the Paleo-Asian Ocean subduction-related melt/fluid–peridotite interaction. Geochim Cosmochim Acta, 140: 435–454
Zou D Y, Zhang H F. 2022. Destruction of Archean lower crust recorded in granulite and pyroxenite xenoliths of Mesozoic basalts from Western Liaoning, North China Craton. Contrib Mineral Petrol, 177: 93
Zou D Y, Zhang H F, Liu D. 2022. Evolution of the Neoarchean lower crust beneath Western Liaoning of the North China Craton: Evidence from U-Pb-Hf-O isotopes in zircon. Precambrian Res, 370: 106555

(Responsible editor: Jianping ZHENG)